

ESRP: ROLE OF HYDROGEN BONDS IN ELECTRON TRANSFER PROCESSES OF TYPE I COPPER PROTEINS

Lincoln-Way East High School ESRP Team 2023

Maxwell Bacon, Madelyn Dryier, Victoria Lucarelli, Andrew Nilsson, Shay Parchem, Dev Patel, Divya Thumu, Liyat Zekarias, Mr. Voliva, Dr. Narayanasami Sukumar, Sahana Sukumar

ABSTRACT

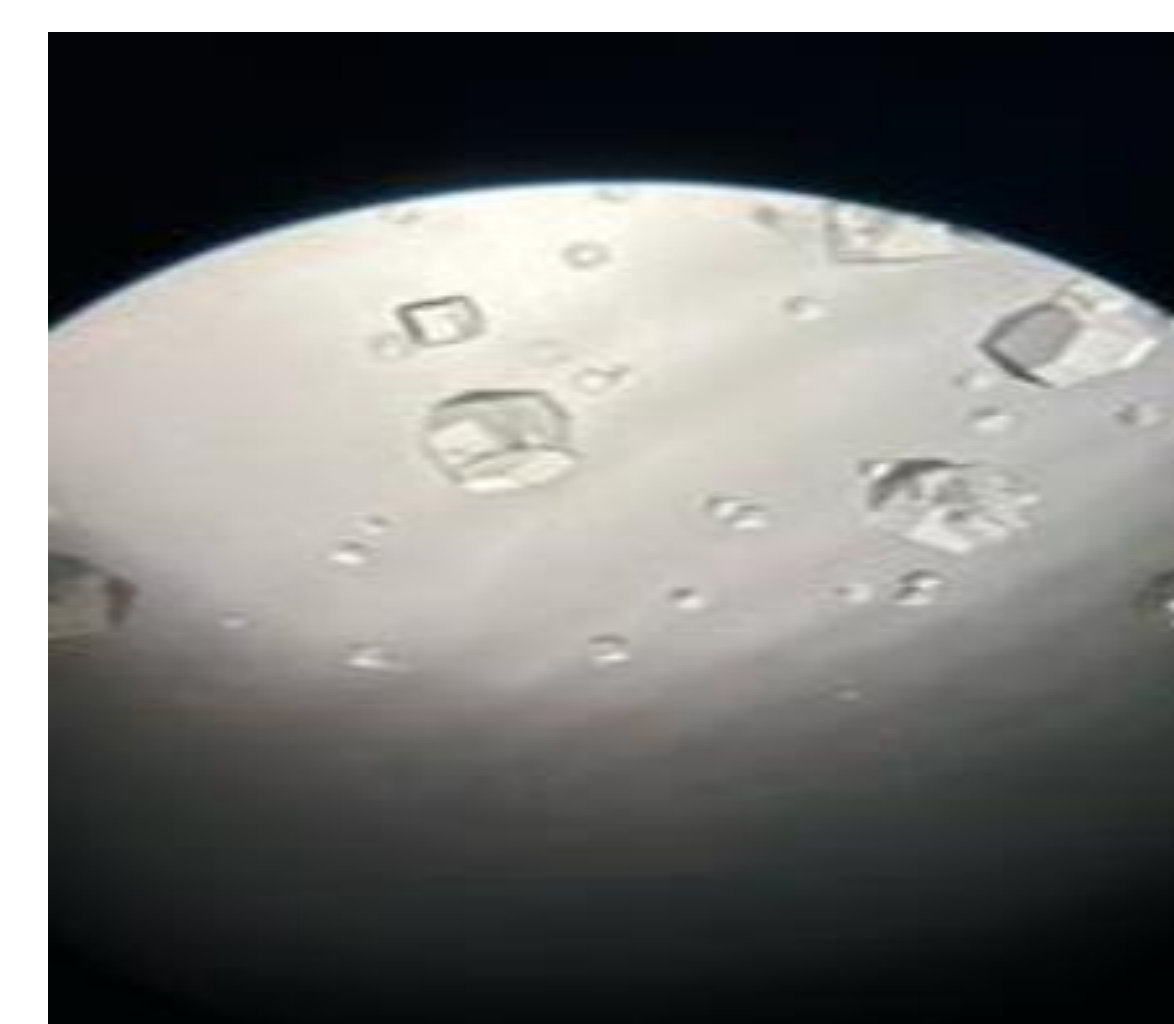
The X-ray crystal structures of several copper proteins that have been solved over the years have enhanced our current understanding in the redox enzymes. These structurally diverse groups of copper proteins perform various important biological activities, such as respiration and photosynthesis. An in-depth structural bioinformatics analysis of these structures was carried out using PDB coordinates of a carefully chosen database of copper proteins to correlate the biological function of the molecules with phylogeny, hydrogen bonds, and their folding. To understand the relationship between the single crystal X-ray crystallography and structural bioinformatics and how they are intertwined with each other, we performed the structure determination of type I copper proteins along with a few model proteins like lysozyme.

MOTIVATION

- Through the extensive research on naturally occurring photosynthesis, several attempts have been made to replace the depletion of fossil fuels with renewable fuels along with environmental concerns. However, one of the reasons such studies were met with limited success was due to the lack of control over the electron transfer (ET) process occurring between the components of the system. To control the ET process, a detailed understanding on the properties of ET process is an absolute necessity. Such information could be obtained by studying the movement of electrons between connected as well as unconnected residues in proteins. Our goal is to elucidate the properties of ET process by studying the role of hydrogen bonds in type I copper proteins in detail so that it can be successfully applied in the field of renewable fuels.

METHODS

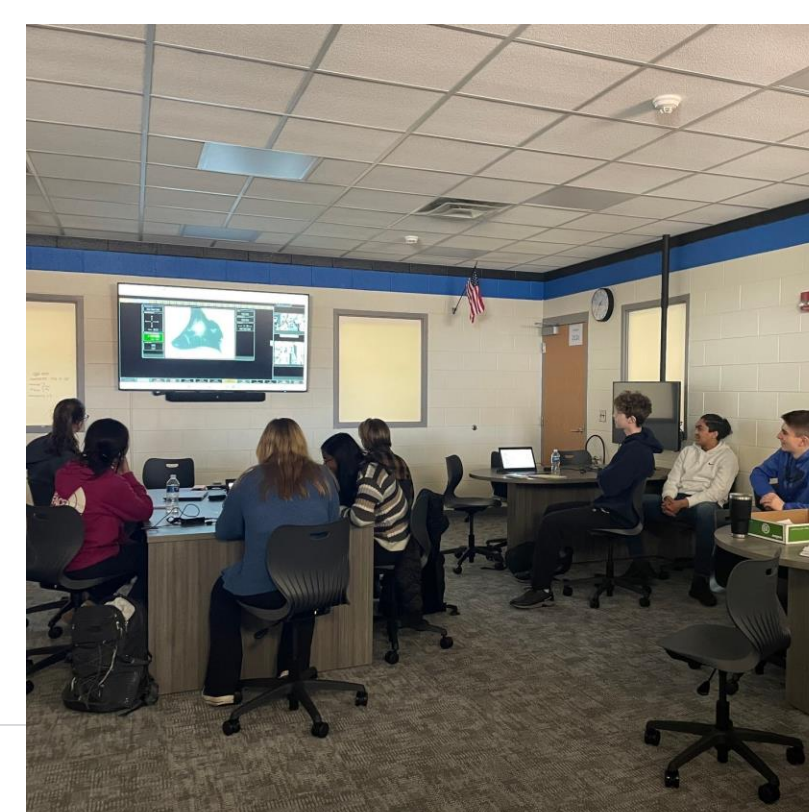
- We sought to map the structure of the protein Lysozyme to understand the process utilized by scientists to add proteins to the PDB.
- First, we crystallized Lysozyme using unique ratios of the neutralizing reagent to liquid lysozyme.
- Then, each member of our team remotely operated the APS on five different crystalized samples of Lysozyme to obtain Lysozyme's diffraction pattern.
- We used the sites RAPD and NECAT in conjunction with the APS to further analyze Lysozyme's structure.



	Overall	Inner Shell	Outer Shell
High resolution limit	1.41	7.72	1.41
Low resolution limit	77.46	77.46	1.43
Completeness	100.0	99.9	100.0
Multiplicity	12.7	9.3	11.6
I/sigma	36.7	88.1	6.2
CC(1/2)	1.000	0.999	0.968
Rmerge	0.038	0.025	0.338
Rmerge (anomalous)	0.036	0.024	0.319
Rmeas	0.040	0.026	0.354
Rmeas (anomalous)	0.039	0.026	0.350
Rpim	0.011	0.008	0.103
Rpim (anomalous)	0.015	0.010	0.141
Anomalous completeness	100.0	100.0	99.9
Anomalous multiplicity	6.7	6.7	5.9
Anomalous correlation	0.176	-0.211	0.061
Anomalous slope	1.087	--	--
Total observations	293082	1718	12926
Total unique	23009	184	1115

OXIDIZED VS REDUCED COPPER PROTEINS

Protein and Ligands/ Folding	Distinct Hydrogen Bonds	Distinct Reduced Bonds
Amicyanin Ligands: HIS53, HIS95, MET98, CYS92 Overall Folding: Composed of a beta-sandwich fold	Oxidized Amicyanin (1AAC) Total Bonds: 58 ILE46(N)-VAL23(O), LYS29(N)-ALA28(O), MET72(N)-HIS53(O), HIS91(N)-HIS56(O), LEU7(N)-PHE57(O), GLY100(N)-TYR86(O), MET98(N)-HIS95(O), VAL58(N)-HIS20(O), TYR90(N)-HIS21(O), LYS74(N)-HIS21(O), MET71(N)-HIS23(O), ALA50(N)-HIS25(O), MET51(N)-HIS25(O), LYS68(N)-HIS29(O), ALA50(N)-HIS26(O), ARG99-PRO96(NE-2-O), ARG99-PRO96(NE-1-O), ARG99-PRO96(NE-2-O), HIS91-HIS24(NE2-O), LYS29-HIS24(NE2-O), ARG99-HIS27(NH2-2-O), ARG99-HIS27(NH2-2-O), LYS27-HIS27(NH2-2-O), LYS27-HIS27(NH2-2-O), LYS27-HIS27(NH2-2-O), ARG99-HIS30(NH1-1-O), ARG99-HIS30(NH2-1-O), ARG99-HIS30(NH1-1-O), LYS29-HIS31(NE2-2-O), LYS29-HIS31(NE2-2-O), ARG99-HIS31(NH1-2-O)	Reduced Amicyanin (2RAC) Total Bonds: 59 VAL23(N)-THR44(O), ASP24(N)-HOH212(O), ILE25(N)-ILE46(O), ALA28(N)-LYS29(O), LYS27(N)-HIS26(O), TYR90(N)-HIS21(O), VAL58(N)-LEU8(O), ASN47(N)-GLU76(O), MET51(N)-HIS21(O), HIS53(N)-MET72(O), HIS55(N)-HIS91(O), PHE57(N)-LEU7(O), VAL58(N)-HIS25(O), MET71(N)-HIS25(O), LYS74(N)-HIS26(O), TYR90(N)-GLY100(O), CYS92(N)-MET98(O), ARG99(N)-HIS24(O), LYS29-HIS28(NE-2-O), ARG48-ASN47(N-OD1), ARG48-GLU75(NH1-OE1), ARG48-HIS28(NH2-O), HIS56-HIS23(NE2-O), HIS56-HIS27(NH2-O), LYS73-HIS27(NE2-O), LYS74-GLU75(NE2-OE2), LYS74-GLU75(NE2-OE2), LYS74-ARG48(NE-O), GLN76-HIS22(NE-O), HIS91-HIS29(NE-O), ARG99-PRO96(NE-O), ARG99-HIS22(NH1-O), ARG99-HIS27(NH1-1-O), ARG99-PRO96(NH2-O), LYS101-ASP98(NE-OD1)
Azurin Ligands: CYS112, GLN5, HIS117, HIS46 Overall Folding: 8 Beta Strands, 1 Alpha Helix	Oxidized Azurin (1DZ7) Total: 50 ASP11(N)-HOH201(O), HIS35(N)-HOH205(O), LYS41(N)-HOH207(O), MET120(N)-HIS117(O), LYS56-HIS203(NE-O)	Reduced Azurin (1DZ0) Total: 51 ASP11(N)-HOH201(O), LYS41 (N)-HOH208(O), LYS41-HIS202(NE-O), MET120(N)-HOH206(O), LYS56-HIS203(NE-O), SER94-ASP9 (N-OD1)
Pseudoazurin Ligands: MET86, CYS78, HIS81, HIS40 Overall Folding: A distorted tetrahedral with an imidazole ring and peptide bond flip	Oxidized Pseudoazurin (1BQR) Total: 74 ASN9(N)-HOH203(O), LYS10(N)-HOH203(O), GLY9(N)-HOH212(O), HIS60(N)-HOH232(O), PHE18(N)-HOH209(O), LYS38(N)-HOH232(O), LYS58(N)-HOH232(O), MET90(N)-HOH232(O), ILE6(N)-HOH227(O), ASN63(N)-HOH232(O), GLY8(N)-HOH232(O), VAL87(N)-GLY85(O), LEU15(N)-GLN121(O), LEU119(N)-LEU119(O), SER58-HIS215(OE-O), TYR82-HIS268(OH-O), ASN9-HIS251(ND2-O), LYS57-HIS28(NE-O), LYS57-HIS28(NE-O), LYS59-HIS29(NE-O), LYS59-HIS29(NE-O), HOH213(NE-O), LYS77-HIS231(NE-O), LYS77-HIS231(NE-O), LYS77-HIS231(NE-O), LYS77-HIS231(NE-O), LYS77-HIS231(NE-O), LYS77-HIS231(NE-O), LYS77-HIS231(NE-O), LYS77-HIS231(NE-O), LYS77-HIS231(NE-O), LYS77-HIS231(NE-O)	Reduced Pseudoazurin (1BQR) Total: 63 LYS10(N)-HOH240(O), ASP130(N)-HOH168(O), PHE18(N)-HOH126(O), LYS38(N)-HOH155(O), ILE60(N)-HOH144(O), ASN63(N)-HOH199(O), GLY8(N)-HOH127(O), VAL87(N)-HOH126(O), LEU119(N)-ALA113(O), SER58-HIS215(OE-O), TYR82-HIS215(OH-O), ASN63-HIS222(OE-O), LYS57-HIS204(NE-O), ASN61-HIS139(ND2-O), LYS77-HIS154(NE-O), LYS77-HIS217(NE-O), ARG114-HIS139(NE-O)
Plastocyanin Ligands: HIS87, HIS37, CYS84, MET92 Overall Folding: 8 Beta Strands	Oxidized Plastocyanin (1BXU) Total: 59 ASN9(N)-HOH36(O), LEU12(N)-HOH341(O), LEU34(N)-HOH308(O), LEU34(N)-HOH345(O), ALA55(N)-HOH345(O), LYS58(N)-HOH305(O), LYS58(N)-HOH334(O), ASP99(N)-HOH305(O), LEU23(N)-HOH329(O), PHE4(N)-HOH349(O), GLY7(N)-HOH327(O), HIS67(N)-CYS84(O), GLY89(N)-HOH332(O), ASN6-CYS84(N-SD), HIS87-ARG88-HIS70(NH1-O)	Reduced Plastocyanin (1BXV) Total: 59 ASN9(N)-HOH309(O), LEU12(N)-HOH306(O), PHE4(N)-HOH312(O), LEU34(N)-HOH319(O), LYS58(N)-HOH322(O), ASP99(N)-HOH326(O), LEU6(N)-HOH326(O), PHE4(N)-HOH345(O), GLY7(N)-HOH346(O), TYR83-HIS76(OH-O), LYS4-HIS381(NE-O), LYS4-ASP8(NE-OD2), LYS3-ASP8(NE-OD2), LYS58-GLU85(NE-OE2), HIS87-CYS84(N-SD), HIS87-HIS311(NE2-O)
Rusticyanin Ligands: HIS5, HIS143, MET148, CYS138 Overall Folding: Core Beta-Sandwich Fold Composed of a 6 and 7 Stranded beta-Sheet	Oxidized Rusticyanin (1A3Z) Total: 63 GLY48(N)-HOH218(O), PHE51(N)-HOH236(O), LYS11(N)-HOH329(O), TYR96(N)-HOH211(O), ALA87(N)-HOH232(O), MET199(N)-HOH232(O), VAL101(N)-HOH210(O), PHE111(N)-HOH226(O), VAL114(N)-HOH265(O), GLY122(N)-HOH214(O), GLY142(N)-HOH212(O), ALA144(N)-HOH221(O), ALA145(N)-HOH210(O), TYR136-PRO202(OH-O), VAL45-GLU55(N-OE1), ALA145(N)-HOH212(O), LYS151(N)-HOH206(O), THR5-HIS292(OE1-O), THR5-HIS288(OE1-O), SER53-GLU55(OE-O), ASN61-HIS238(OE2-O), ASN60-HIS228(OE2-O), ASN60-HIS279(NE2-O)	Reduced Rusticyanin (1A3Z) Total: 64 THR63(N)-ASP29(O), LYS81(N)-HOH234(O), GLY82(N)-HOH212(O), TYR96(N)-HOH209(O), ALA97(N)-HOH208(O), MET99(N)-HOH220(O), VAL101(N)-HOH208(O), THR109(N)-PHE87(O), VAL114(N)-HOH230(O), GLY122(N)-HOH211(O), GLY142(N)-HOH210(O), ALA144(N)-HOH214(O), ALA145(N)-HOH210(O), TYR136-PRO202(OH-O), VAL45-GLU55(N-OE1), ASN61-ASN61(N-OD1), ASN61-HIS238(NE2-O), ASN60-HIS218(ND2-O), ASN60-HIS234(ND2-O), GLN139-ASP98(NE-OD1), HIS48-HIS246(NE2-O)

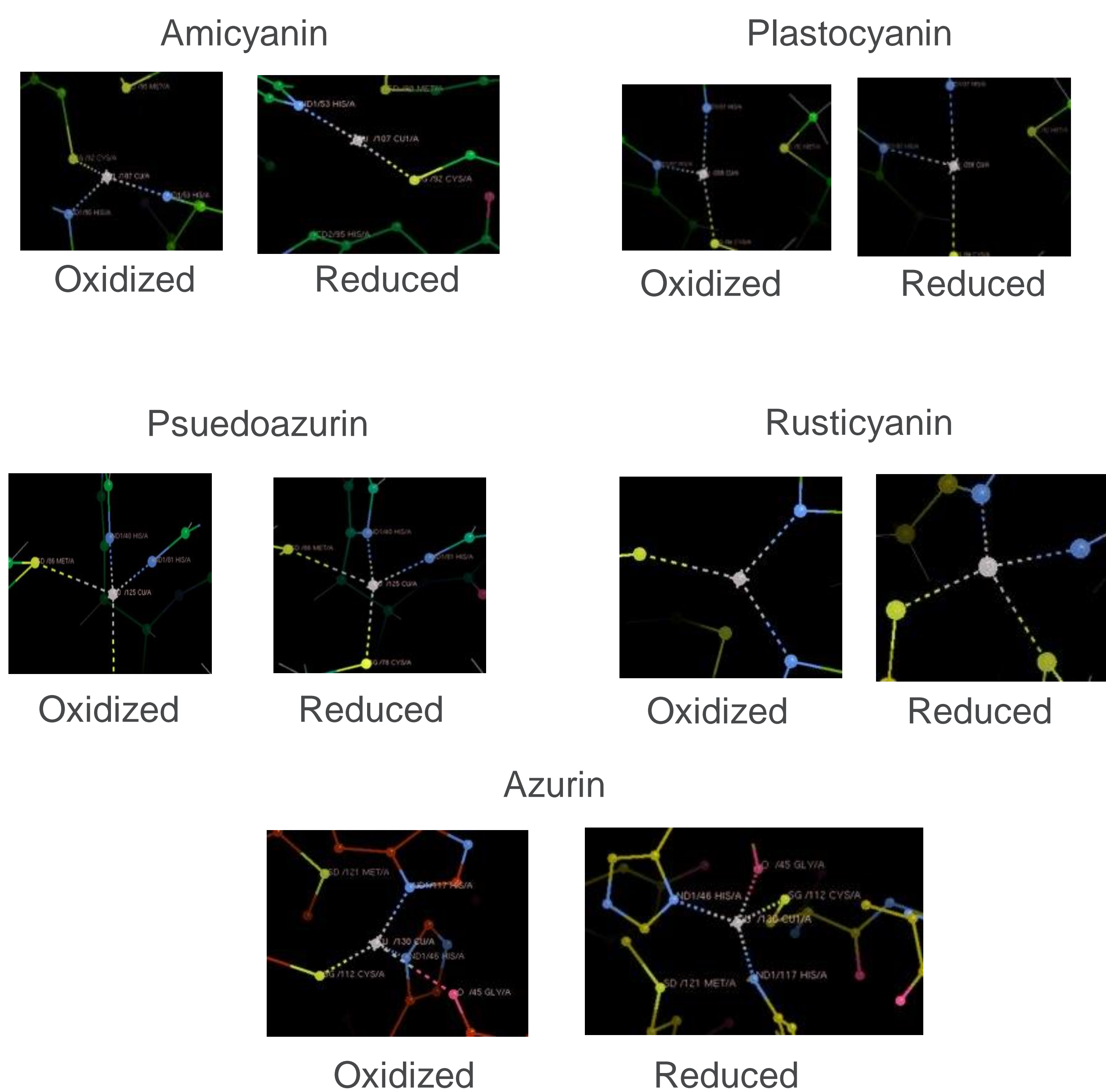


- COOT was used to center each protein around its central copper atom to focus the analysis of hydrogen bonds on the atoms surrounding the central copper atom.
- CCP4MG was used to find the hydrogen bonds of PDB files focused using COOT.
- What if was used to confirm that the methods used to calculate hydrogen bonds using CCP4MG produced correct data.



COPPER SITES

- Our control protein, Amicyanin, had 4 residues: 2 HIS, 1 CYS, and 1 MET
- Based off of this information, we obtained the remainder of our proteins so each of them consistently had 2 HIS and 1 CYS and were similar to the copper site of Amicyanin



MAJOR ACCOMPLISHMENTS

- Visited Argonne to learn the function of the APS.
- Virtually controlled the APS to analyze five prepared samples of crystalized lysozyme and collect diffraction data.
- Successfully crystallized lysozyme in two trials
- 8 Type-1 Copper proteins were analyzed and a correlation between hydrogen bonding and oxidation states was found.
- Created programs to sort through and format hydrogen bonding data so it could be efficiently analyzed.
- Based on the difference in the total hydrogen bonds there was a difference in the bonds amongst the ligand residues, HIS being the main determinant. When the oxidized or reduced state had an extra bond involving HIS, it had more total bonds.

FUTURE DIRECTIONS

- The knowledge of the significance of the presence of the HIS copper ligand on oxidation state, increases humanity's knowledge of how oxidation state is related to hydrogen bonding.
- By knowing more about the significance of the presence of the HIS ligand copper ligand, more gaps in knowledge are filled which can be used to support other research and innovations related to biological processes.

REFERENCES

- Sukumar, N. *PNAS*. 107,15 (2010): 6817-22.
- Sukumar, N. *Biochimie* vol. 95,5 (2013): 976-88.
- PDB Files Used: 1AAC, 5N4L, 2RAC , 1RCY , 1A3Z , 1BXU , 1BXV , 1DYZ , 1DZ0, 1BQR , 1BQK, 1JER, 2BHF
- Code: <https://github.com/orgs/LWE-ESRP-22-23/repositories>